Comparison of structure and luminescence between β-$FeSi_2$ /Si (100) and β-$FeSi_2$ /Si (111) heterojunctions prepared by pulsed laser deposition

S. C. XU, S. B. GAO, M. LIU, C. YANG, C. S. CHEN, S. Z. JIANG, X. G. GAO, Z. C. SUN, B. Y. MAN*
College of Physics and Electronics, Shandong Normal University, Jinan 250014, P.R. China

The β-$FeSi_2$/Si (100) and β-$FeSi_2$/Si (111) heterojunctions were prepared by growing β-$FeSi_2$ thin films on Si (100) and Si (111) substrates respectively with pulsed laser deposition (PLD) method. Crystalline structures of the films were measured by X-ray diffraction (XRD) and Fourier transform infrared spectroscopy (FTIR). The β-$FeSi_2$ films on Si (100) had a more orderly structure than those on Si (111). Surface properties and the elemental composition in the depth direction of β-$FeSi_2$/Si heterojunctions were characterized with scanning electron microscopy (SEM) and X-ray photoelectron spectroscopy (XPS), respectively. For both kinds of the heterojunctions, a clear interface between the films and substrates was obtained. The distinct light-emitting was achieved on β-$FeSi_2$/Si heterojunctions at 30 K, and the β-$FeSi_2$ /Si (100) heterojunction performed a better photoluminescence than β-$FeSi_2$ /Si (111) heterojunction.

(Received November 22, 2011; accepted February 20, 2012)

Keywords: Pulsed laser deposition, Photoluminescence, β-$FeSi_2$

1. Introduction

In the past decade, semiconducting β-$FeSi_2$ has attracted much attention due to its theoretical direct band gap of 0.85 eV, which fits transmission window of silica based on optical fiber [1-5]. It was also further studied as a candidate for application to the optoelectronics devices with the well compatibility with silicon technology. Because of the large absorption coefficient ($\alpha>10^{-5}$ cm^{-1} at 1.0 eV), β-$FeSi_2$ is expected to be a candidate for a new solar cell material [6, 7]. Furthermore, it has superior features such as chemical stability, non-toxicity and its components are abundant on the earth, which as well favor the use of β-$FeSi_2$ as a new type of environmentally friendly material. The semiconductor silicon element has a considerable role within the technology of photovoltaics. Silicon-based photovoltaic devices are preferable due to their stable chemical properties and their consistency with the technology of microelectronics [8].However, in contrast to the excellent theoretical properties of β-$FeSi_2$ material, few practical results has been achieved in experiments. Many growth methods have been explored to fabricate the β-$FeSi_2$ films on Si substrate, including reactive deposition epitaxy (RDE) [9, 10], ion beam synthesis (IBS) [11, 12], solid phase epitaxy (SPE) [13, 14], molecular beam epitaxy (MBE) [15-17] and pulsed laser deposition (PLD) [18, 19], etc. These efforts contributed to the improvement of the β-$FeSi_2$ film quality and the high quality β-$FeSi_2$ film has been prepared in our previous work [18]. However, it is still very hard to prepare the high quality β-$FeSi_2$ /Si heterojunction owing to un-sharp interface between the β-$FeSi_2$ films and the Si substrates, which was thought to be induced by the significant interdiffusion of Fe and Si atoms due to the high temperature in the β-$FeSi_2$ formation process.

In this study, we firstly fabricated a thin β-$FeSi_2$ template layer by introducing iron on silicon substrates at low temperature and then deposited β-$FeSi_2$ films on the template layer by using PLD method. The interdiffusion of Fe and Si at the interface was effectively prevented by the β-$FeSi_2$ template layer, and the β-$FeSi_2$ /Si (100) and β-$FeSi_2$ /Si (111) heterojunctions with a clear interface were obtained. The crystalline structure and the morphology of the two kinds of heterojunctions were also compared, and the distinct photoluminescence was realized on both kinds of heterojunctions.

2. Experimental procedure

For the preparation of crystalline β-$FeSi_2$ films, the Fe target (99.999%, dimensions 5×4×0.3 cm) and the β-$FeSi_2$ ceramic (99.9%, dimensions 5×5×0.3 cm) were initially cleaned by laser ablation for 3 min under vacuum conditions to remove the surface contaminants. The p-type (100 orientation and resistivity 0.5-0.7 Ω·cm) and p-type (111 orientation and resistivity 0.7-0.9 Ω·cm) substrates were cleaned with organic solvents and dipped in a dilute HF (HF: H_2O = 2:40) solution for 1 min to get rid of the native silicon oxide. The β-$FeSi_2$ /Si (111) heterojunctions were formed in two steps. First, a thin β-$FeSi_2$ template layer was formed on the Si substrate prior to the thick film

deposition. A thin Fe layer was deposited on Si substrate by a Nd:YAG pulsed laser with a wavelength of 1064 nm with a base pressure of 2×10^{-5} Pa at 300 ℃. The deposited Fe atoms reacted with the diffused Si atoms from the underlying Si substrate to produce a β-$FeSi_2$ layer. Then, the thick film deposition was carried out by a KrF excimer laser with a wavelength of 248 nm at 650 ℃. The coating duration of the β-$FeSi_2$ was set to be 10, 15 and 20 min, respectively. For both lasers, the laser fluence was 7 J/cm^2 and the repetition rate was 10 Hz. The distance between the targets and the substrates was 40 mm.

The crystalline structures of the thin films were characterized by using XRD (A Rigaku D/max-rB X-ray diffraction meter with Cu Kα-line) and FTIR (TENSOR27). The surface morphology of β-$FeSi_2$/Si heterojunctions were investigated with SEM (Hitachi S-570) and field emission scanning electron microscopy (FSEM, ZEISS-SUPRA55). The XPS experiments were performed in an electron spectrometer (Escalab MKII) at base pressure of 2×10^{-8} Pa in chamber. The photoelectrons were excited with an X-ray source (Mg Kα; 1253.6 eV). The depth profiling was carried out by sputter erosion at 45° applying Ar^+ beam of 3 keV energy and current density 16 μA cm^{-2}. Luminescence was analyzed by a 25 cm focal length monochrometer (Ritsu, MC-25N) and detected by a liquid-nitrogen-cooled InP/InGaAsP photo-multiplier (Hamamatsu Photonics R5509-72).

3. Results and discussion

In this study, β-$FeSi_2$ films with 3 different thicknesses were grown by PLD on Si (100) and Si (111) substrates. Fig. 1 shows the X-ray diffraction patterns of β-$FeSi_2$ films on Si (100). Apart from the Si (400) peak, the β-$FeSi_2$ (400), (422), (600) and (800) peaks are observed [20], and the (100)-orientated peaks of β-$FeSi_2$ are dominant, indicating that an epitaxial relationship with the Si (100) substrate is obtained. The XRD patterns of β-$FeSi_2$ /Si (111) heterojunctions are shown in Fig. 2. It can be seen that the films on Si (100) and Si (111) have different crystal orientations. The β-$FeSi_2$ films on Si (111) present the random orientations. Apart from the Si (111) peak, the pronounced β-$FeSi_2$ (202)/ (220), and some weak peaks such as β-$FeSi_2$ (313), (422), (040), (041), (133) and (024) appear [20]. This result indicates that the films on Si (100) have a more orderly texture than those on Si (111), which were independent of film thickness. Since the XRD patterns of these two kinds of the heterojunctions are not thickness-related, the films grown for 15 min were analyzed only in the following.

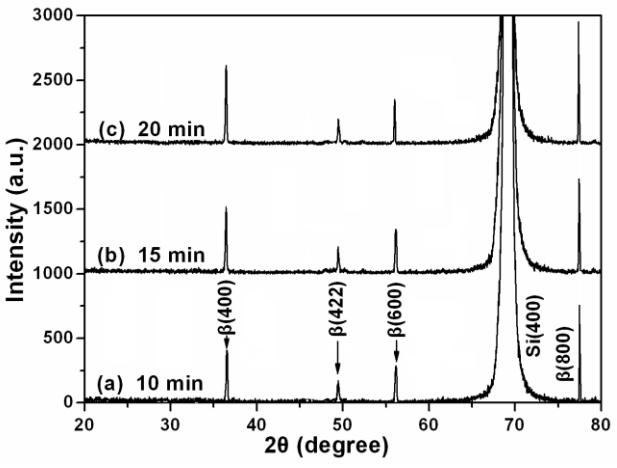

Fig. 1. XRD patterns of the β-$FeSi_2$/Si (100) heterojunction. (a) t=10 min,(b) t=15min, (c) t=20min.

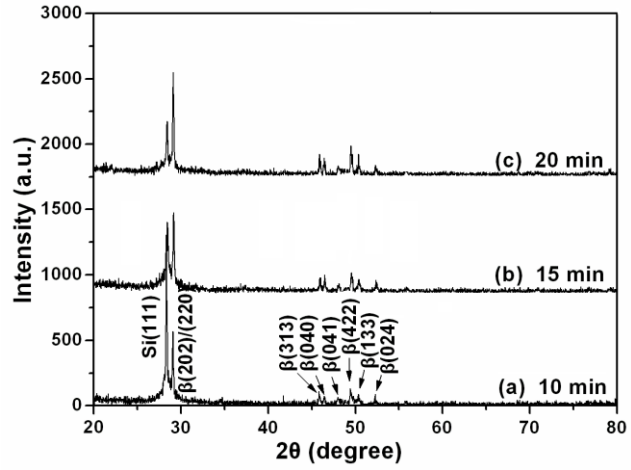

Fig. 2. XRD patterns of the β-$FeSi_2$/Si (111) heterojunction. (a) t=10 min,(b) t=15min, (c) t=20min.

The FTIR spectra of the films deposited on Si (100) and on Si (111) are shown in Fig. 3(a) and (b), respectively. As can be seen from the Fig. 3, five peaks are located at average wave numbers of 263, 297, 311, 345, and 425 cm^{-1}, which are all related to the infrared vibrations of β-$FeSi_2$ [21]. We further confirm that the β-$FeSi_2$ films were successfully fabricated on both Si (100) and (111) substrates. According to the experimental spectra offered by Guizzetti, et al [22], the features at about 300-400 cm^{-1} are expected to originate from the counter phase motion of Fe and Si atoms and the numbers lower than 300 cm^{-1}, detected at about 263 cm^{-1}, 297 cm^{-1}, are related to the vibration of the Fe–Fe atoms. The one at a higher frequency of 425 cm^{-1} is attributed to the motion of the Si–Si atoms. By comparing the IR spectra of the two samples, it is found that the peaks of the film on Si (100) are sharper and higher than those on Si (111). This result indicates that the crystalline quality of films on Si (100) is better than that on Si (111).

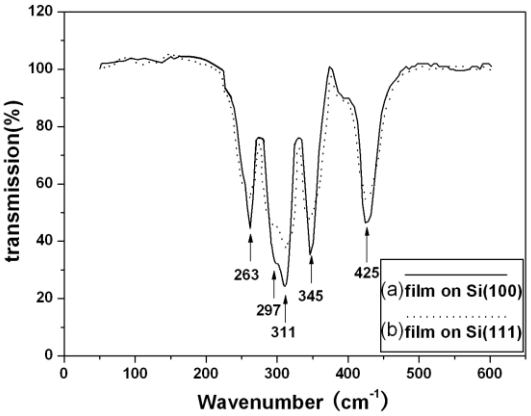

Fig. 3. FTIR spectra of the films deposited on Si (100) (a) and on Si (111) (b).

Fig. 4(a) and (b) shows the surface morphologies of the films grown on Si (100) and on Si (111) substrates, respectively. The film surface in Fig. 4(a) is continuous and uniform, no holes and clusters are found even in a large area, suggesting the high quality interfacial connection. The film surface in Fig. 4(b) shows rill-like folds and some agglomerations with various shapes and sizes. The cross sectional FSEM images of the β-$FeSi_2$/Si (100) and β-$FeSi_2$/Si (111) heterojunctions are also given in Fig. 4(c) and (d), respectively. Fig. 4(c) exhibits a smooth interface line between the upper β-$FeSi_2$ layer and the Si (100) substrate below. The upper layer adheres to the Si (100) substrate completely and no gaps exist in the interface, suggesting that an excellent β-$FeSi_2$ /Si (100) heterojunction was obtained. Fig. 4(d) also shows a clear interface between β-$FeSi_2$ layer and Si (111) substrate. Some agglomerations are on the interface of β-$FeSi_2$ layer and the Si (111) substrate. These agglomerations are thought to be formed due to the lattice-matching strain or the difference in surface energy between the film and the substrate. It is interesting to note that the thickness of β-$FeSi_2$ layer on Si (100) and on Si (111) is quite different, even though the depositional conditions are the same. The β-$FeSi_2$ layer on Si (111) is as thick as 100 nm, while the layer on Si (100) substrate is about 80 nm. The β-$FeSi_2$ layer on Si (111) is much thicker than that on Si (100). The different thicknesses of the films can be attributed to the different epitaxial relationship. The lattice mismatch for the epitaxial relationship of β-$FeSi_2$ (100)/Si (100) is 1.8%, while the lattice mismatch between β-$FeSi_2$ (202)/(220) and Si (111) can be as much as 5% [23]. The large lattice misfit for β-$FeSi_2$ on Si (111) generates many misfit dislocations near the interfaces and thus forms many defects. Usually, the defects possessing a large number of dangling bonds may act as nucleation centers for the precipitation. We suggest that the presence of the dangling bonds at the defects will have promoted the absorption of the sputtering atoms. The adsorption effect of the defects reduces the reflection of the sputtering atoms, resulting in the thickness difference of the films. On the other hand, the films epitaxially grown on Si(100) substrate have the preference of two-dimension (2-D) growth over three-dimension (3-D) growth due to small lattice mismatch when compared with Si (111) [24]. That is reasonable to explain that the surface morphology on Si (100) is much smoother than that on Si (111).

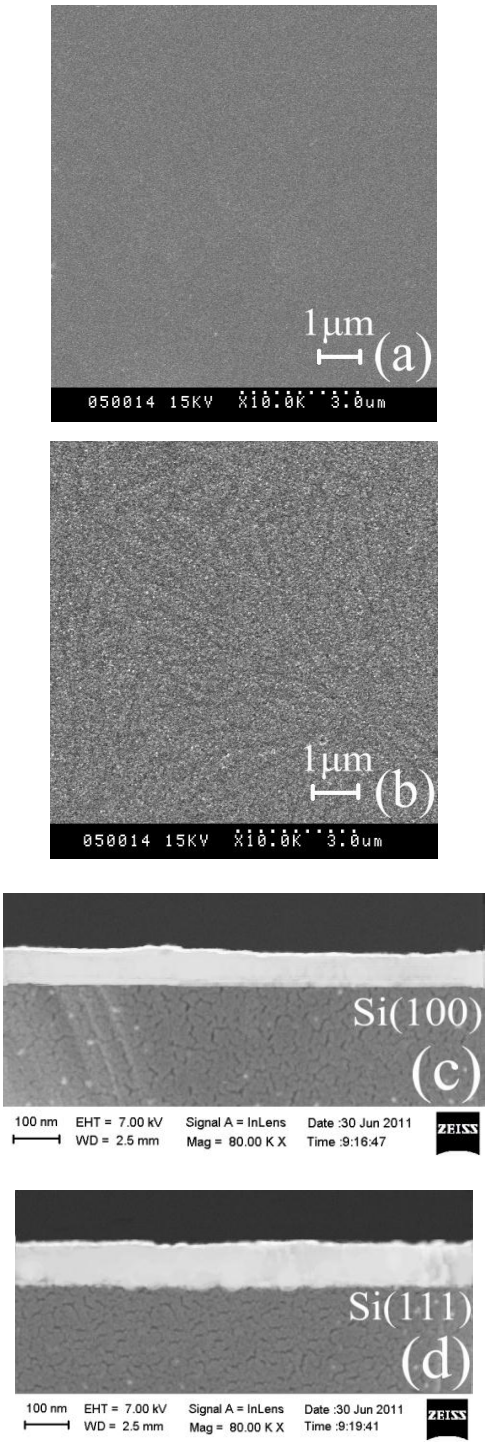

Fig. 4. SEM images of the films deposited on Si (100) (a) and on Si (111) (b); Cross sectional FSEM image of the β-$FeSi_2$/Si (100) heterojunction (c) and the β-$FeSi_2$/Si (111) heterojunction (d).

The composition ratio of Fe and Si in the β-$FeSi_2$ films on Si (100) and Si (111) is measured in the depth direction by XPS, shown in Fig. 5(a) and (b), respectively. Depth profiling was performed up to about 100 nm after 120 min Ar^+ sputtering. Both profiles are plateau-like and exhibit iron concentrations of about 30 % and the corresponding silicon concentration of about 70 % before 80 min Ar^+ sputtering. The ratio of Fe and Si is found to be about 1:2, which corresponds to stoichiometric β-$FeSi_2$. We note that the plateau of the β-$FeSi_2$ /Si (111) heterojunction is broader than that of β-$FeSi_2$ /Si (100) heterojunction. It is suggested that the β-$FeSi_2$ layer on Si (111) is thicker than that on Si (100). This result is well consistent with the cross sectional FSEM images. As can be seen in Fig. 5(a), the iron concentration drop to zero quickly, while in Fig. 5(b) it takes about 25 min to decease to zero. It is indicated that for the β-$FeSi_2$ /Si (111) heterojunction there exists an iron-insufficient transitional layer on the interface region. It can be speculated that due to the insufficiency of iron, the iron vacancy-related defects are likely to form in transitional layer.

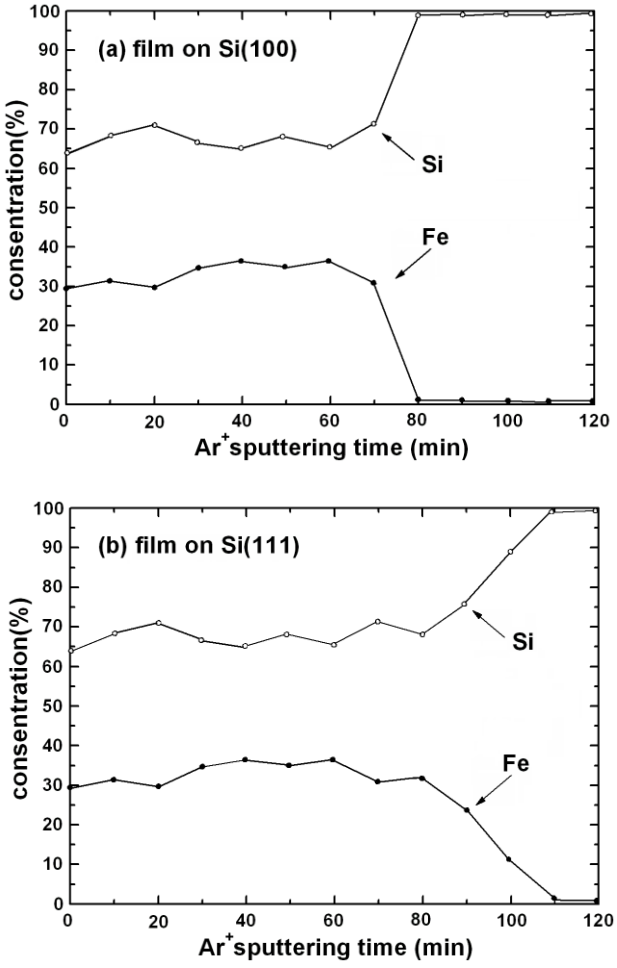

Fig. 5. Dependence of iron and silicon concentration on the Ar^+ sputtering time for the β-$FeSi_2$/Si (100) heterojunction (a) and the β-$FeSi_2$/Si (111) heterojunction (b).

The PL spectra measured at 30 K for the samples grown on Si (100) and Si (111) substrates are shown in Fig. 6 (a) and (b), respectively. A distinct peak is seen at around 0.81 eV for both cases, which can be attributed to the radiative recombination of electron hole pairs in β-$FeSi_2$ films [25]. The peak at around 1.1 eV is associated with the bound exciton of Si, and the weak peak at about 0.87 eV is from the dislocation-related D-line emission [26]. Both spectra have similar characteristics for the peak position and the shape. Moreover, it can be seen that PL intensity of the β-$FeSi_2$ /Si (100) heterojunction is higher than that of the β-$FeSi_2$ /Si (111) heterojunction. The weaker PL of the films on Si (111) is considered to be attributable to more defects due to the larger lattice mismatch in the β-$FeSi_2$ /Si (111) heterojunction than in the β-$FeSi_2$ /Si (100) heterojunction. The defects are considered to act as the nonradiative recombination centers, leading to degradation of the PL intensity.

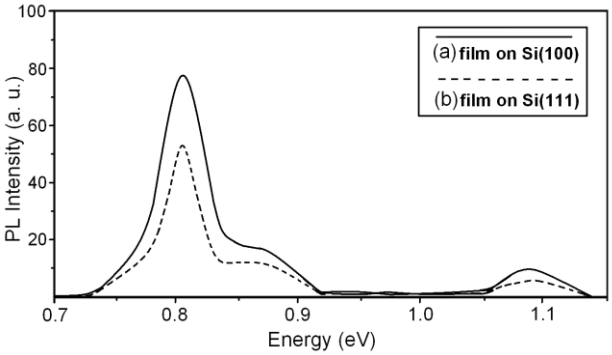

Fig. 6. PL spectra of the β-$FeSi_2$/Si (100) heterojunction (a) and the β-$FeSi_2$/Si (111) heterojunction (b).

4. Conclusions

The β-$FeSi_2$ /Si (100) and β-$FeSi_2$ /Si (100) heterojunctions were obtained by coating β-$FeSi_2$ films on a preformed thin template layer with a pulsed laser deposition technique. For both kinds of the heterojunctions, a clear interface between the films and substrates was obtained. Though the depositional condition is the same, the β-$FeSi_2$ /Si (100) heterojunction have a more orderly texture, better morphology and more smooth interface than the β-$FeSi_2$ /Si (111) heterojunction. The distinct photoluminescence was achieved on β-$FeSi_2$ /Si heterojunctions at 30 K. The film on Si (100) performed a better photoluminescence due to the less defects related to the lattice mismatch. In conclusion, the Si (100) is more suitable for β-$FeSi_2$ /Si heterojunctions than Si (111).

Acknowledgements

The authors are grateful for the financial support of the National Natural Science Foundation of China (11047161, 10874103), the Provincial Natural Science

Foundation of Shandong (Y2007A05) and the Postdoctoral Innovation Projects of Shandong (200903036).

References

[1] D. Leong, M. Harry, K. J. Reeson, K. P. Homewood, Nature **387**, 686 (1997).
[2] C. Li, H. K. Lai, S.Y. Chen, T. Suemasu, F. Hasegawa, J.Cryst. Growth **290**,197 (2006).
[3] Y. Ugajin, M. Takauji, T. Suemasu, Thin Solid Films **508**, 376 (2006).
[4] K. Akiyama, Y. Hirabayashi, S. Kaneko, T. Kimura, S. Yokoyama, H. Funakubo, J. Cryst. Growth **289**, 37 (2006).
[5] S. Murase, T. Sunonara, T. Suemasu, J. Cryst. Growth **301**, 676 (2007).
[6] T. Yoshitake, G. Shiraishi, K. Nagayama, Appl. Surf. Sci.**197**, 379 (2002).
[7] N. Dmitruk, L. Dozsa, S. Mamykin, O. Kondratenko, G. Molnar, Vacuum **84**, 238 (2010).
[8] B. Tatara, K. Kutlu, M. Ürgen, Surf. Coat. Technol. **201**, 8373 (2007).
[9] K. Takakura, T. Suemasu, F. Hasegawa, Thin Solid Films **369**, 253 (2000).
[10] N. Vouroutzis, T. T. Zorba, C. A. Dimitriadis, K. M. Paraskevopoulos, L. Dózsa, G. Molnár, J. Alloys Compd. **448**, 202 (2008).
[11] K. Shimure, K. Yamaguchi, M. Sasase, H. Yamamoto, S. Shamoto, K. Hojou, Vacuum **80**, 719 (2006).
[12] K. Yamaguchi, K. Shimura, H. Udono, M. Sasase, H. Yamamoto, S. Shamoto, K. Hojou, Thin Solid Films **508**, 367 (2006).
[13] N. Onda, H. Sirringhaus, S. Goncalves-conto, C. Schwarz, S. Zehnder, H. Kanel, Appl. Surf. Sci. **73**, 124 (1993).
[14] N. Vouroutzis, T. T. Zorba, C. A. Dimitriadis, K. M. Paraskevopoulos, L. Dózsa, G. Molnár, J. Alloys Compd. **393**, 167 (2005).
[15] T. Sunohara, K. Kobayashi, T. Suemasu, Thin Solid Films **508**, 371 (2006).
[16] H. Kakemoto, T. Higuchi, H. Shibata, S. Wada, T. Tsurumi, Thin Solid Films **515**, 8154 (2007).
[17] S. Matsumura, K. Ochiai, H. Udono, F. Esaka, K. Yamaguchi, H. Yamamoto, K. Houjo, Physics Procedia **11**, 174 (2011).
[18] B. Y. Man, S. C. Xu, C. Yang, M. Liu, S. Z. Jiang, Y. Y. Ma, C. S. Chen, A. H. Liu, X. G. Gao, C. C. Wang, B. Hu, Appl. Surf. Sci. **257**, 6321 (2011).
[19] A. Yokotani, Y. Okazaki, K. Nurulhusna, M. Tode, Y. Takigawa, Optical Materials **32**, 759 (2010).
[20] Powder Diffraction File, Card 20-352, Joint Committee on Powder Diffraction Standards, published by International Center for Diffraction Data 1989.
[21] D. Gong, D. S. Li, Z. Z. Yang, M. H. Wang, D. R. Yang, Appl. Surf. Sci. **254**, 4875 (2008).
[22] G. Guizzetti, F. Marabelli, M. Patrini, P. Pellegrino, B. Pivac, L. Miglio, V. Meregalli, H. Lange, W. Henrion, V. Tomm, Phys. Rev. B **55**, 14290 (1997).
[23] J. E. Mahan, V. L. Thanh, J. Chevrier, I. Berbezier, J. Derrien, R.G. Long, J. Appl. Phys. **74**, 1747 (1993).
[24] Y. Nakamura, S. Amari, N. Naruse, Y. Mera, K. Maeda, M. Ichikawa, Cryst. Growth Des. **8**, 3019 (2008).
[25] M. G. Grimaldi, C. Bongiorno, C. Spinella, E. Grilli, L. Martinelli, M. Gemelli, D. B. Migas, Leo Miglio, M. Fanciulli, Phys. Rev. B **66**, 085319 (2002).
[26] C. Li, H. Lai, S. Chen, T. Suemasu, F. Hasegawa, J. Cryst. Growth **290**,176 (2006).

*Corresponding author: byman@sdnu.edu.cn